Chapter 2

# Types of Nonlinear Interactions between Plasmonic-Excitonic Hybrids

*Kaweri Gambhir and Agnikumar G. Vedeshwar*

## Abstract

The unique ability of plasmonic structures to concentrate and manipulate photonic signals in deep sub-wavelength domain provides new efficient pathways to generate, guide, modulate and detect light. Due to collective oscillations exhibited by the conducting electrons of metallic nanoparticles, their local fields can be greatly enhanced at the localized surface plasmon resonance (LSPR). Hence, they offer a versatile platform, where localized surface plasmons can be tuned over a broad range of wavelengths by controlling their shape, size and material properties. It has been realized that plasmonic excitations can strengthen nonlinear optical effects in three ways. First, the coupling between the incident beam of light and surface plasmons results in a strong local confinement of the electromagnetic fields, which in turn enhances the optical response. Second, the sensitivity of plasmonic excitations toward the dielectric properties of the metal and the surrounding medium forms the basis for label-free plasmonic sensors. Finally, the excitation and relaxation dynamics of plasmonic nanostructures responds to a timescale of femtoseconds regime, thus allowing ultrafast processing of the incident optical signals. This chapter aims to discuss all the aforementioned interactions of plasmons and their excitonic hybrids in detail and also represent a glimpse of their experimental realizations.

**Keywords:** plasmon, exciton, nonlinear interactions, resonant interactions, nonresonant interactions

## 1. Introduction

The basic requirement for the realization of ultrafast photonic switches, optical limiters and modulators is substantial third-order optical nonlinearity of materials at low light powers [1–3]. However, most of the natural materials possess insignificant nonlinearity in the low light regime [4]. Therefore, design and fabrication of nanoengineered hybrid materials with tunable absorption/emission spectra and considerable third-order optical nonlinearity are a topic of global research [3, 5–7].

It has been realized that plasmonic oscillations can enhance nonlinear optical (NLO) effects majorly in three ways.

First, the coupling between the incident beam and surface plasmons results in a strong local confinement of the electromagnetic fields which in turn enhances the

optical response [8, 9]. This phenomenon forms the basis of surface-enhanced Raman scattering (SERS), where plasmonic excitations arising from metal nanosurfaces are used to boost otherwise weak Raman process by several orders of magnitude [10, 11].

Second, the sensitivity of plasmonic excitations towards the dielectric properties of the metal and the surrounding medium forms the basis for label-free plasmonic sensors. Even the slightest alterations in the refractive index of the environment surrounding the metal surface leads to considerable modifications in the resonance of the plasmonic nanostructures [12, 13]. In nonlinear optical phenomena, this extraordinary sensitivity may be effectively used to control photon-photon interaction. Where, the control beam may be used to modify the dielectric properties of the medium, which in turn would change the plasmonic resonances of the propagating signal beam [14].

Finally, the excitation and relaxation dynamics of plasmonic nanostructures responds to a timescale of femtoseconds regime, thus allowing ultrafast processing of the incident optical signals [15, 16]. This property of plasmonic nanostructures may be conveniently exploited to attain an ultrahigh switching contrast in *All Optical Switching* applications.

Thus, the confinement of surface plasmons in the nanoscale regime not only provides a flexible means of tailoring the optical properties of plasmonic nanostructures but also allows hybridization of metal nanostructures with other molecules such as semiconductors, organic molecules, inorganic molecules [17, 18]. Exclusively, plasmonic-organic hybrids have gathered a lot of attention due to their flexible and versatile interaction mechanisms which can be further fine-tuned to achieve the desired photonic characteristics. Plasmon coupled organic molecules have led to substantial progress in high-throughput DNA detection [19, 20], bio-imaging [21], drug delivery [22], photovoltaic [23] and light-emitting diodes [24], surface-enhanced Raman spectroscopy [11], nanoscale lasers [25], ultrasensitive chemical and biological sensors [26].

## 2. Nonlinear light-matter interactions

The interaction of light with matter can be broadly classified in two categories (a) linear interaction (weak light regime) and (b) nonlinear interaction (intense light regime). When the intensity of the incident beam is so high that it is nearly equal to the internal electric field of the atom then the absorption coefficient and the real and imaginary part of the nonlinear refractive index ($n$) and absorption coefficient ($\beta$) of the material become a function of the incident intensity or electric field [27]. Such that, polarization of the materials tends to behave nonlinearly with the incident electric field (Eq. (1)).

$$P_i = \varepsilon_0 \chi^{(1)}_{ijk} E_j + \varepsilon_0 \chi^{(2)}_{ijk} E_j E_k + \varepsilon_0 \chi^{(3)}_{ijk} E_j E_k E_l + \ldots \tag{1}$$

where, $\varepsilon_0$ denotes permittivity of free space, $P$ is electric polarization, $\chi$ symbolizes electric susceptibility tensor, $\varepsilon_0 \chi^{(1)}_{ijk} E_j$ is the linear polarization, $\varepsilon_0 \chi^{(2)}_{ijk} E_j E_k$ depicts second order nonlinearity, $\varepsilon_0 \chi^{(3)}_{ijk} E_j E_k E_l$ is the third order nonlinearity and so on.

Hence, in comparison with the linear interaction, during nonlinear interaction superposition principle gets violated, light can alter its frequency as it passes through a

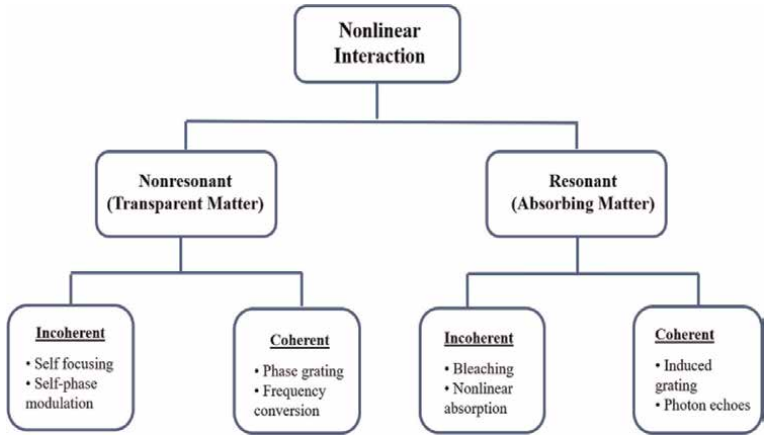


**Figure 1.**
*Schematic representation of nonlinear interaction of light with matter [27].*

NLO material and photons start interacting with each other within the confines of a NLO medium [27, 28]. The nonlinear interactions of light are further classified as resonant and nonresonant interactions (**Figure 1**).

The nonresonant or elastic interactions are the ones in which the incident light is not absorbed by the material (sample). Therefore, these interactions can be described using nonlinear polarization in terms of the Maxwell equations, whereas, in case of resonant interactions or coherent interactions emission/absorption of light inside the material takes place. The density matrix formalism is hence used to evaluate such interactions as discrete structure of the energy levels inside matter and their phase dependent occupation during the light wave period are important to be considered in these interactions [27, 28].

When high intensity light is incident on a medium, based on its inherent response scattering, refraction or absorption takes place. This in turn alters the transmittance of the medium as a function of the input light intensity and is termed as nonlinear light absorption or nonlinear light transmission. However, at very high intensities, the probability of the medium absorbing more than one photon before relaxing to the ground state becomes prominent.

A few phenomena that control nonlinear light transmission are listed below.

## 2.1 Saturable absorption

Saturable absorption (SA) is the mechanism in which the absorption of light is inversely proportional to light intensity. That is at sufficiently high intensities of the incident beam, if the rate of excitation of atoms is greater than their decay rate then the ground state gets depleted resulting in a saturable absorption. Further, this phenomenon critically depends on the absorption range of the material, its dynamic response and saturation intensity.

The steady state rate equation for saturable absorption is denoted by Eq. (2).

$$\frac{dN}{dt} = \frac{\sigma I}{h\nu}\left(N_g - N\right) - \frac{N}{\tau} \tag{2}$$

where, $N$ is the number of excited state molecules, $N_g$ is the undepleted ground state concentration, $\sigma$ is termed as absorption cross section, $h\nu$ is the photon energy, and $\tau$ is the lifetime of the excited state population.

Assuming that the absorption coefficient and $\alpha$ is proportional to the ground state population. Saturable absorption finds application in passive mode locking and Q-switching of lasers and optical signal processing [27, 28].

### 2.2 Two-photon absorption

When simultaneous absorption of two photons from an incident beam causes a transition of atoms/molecules of a material from ground state to a higher energy level, this phenomenon is termed as two-photon absorption (TPA). The intermediate level in this case is a virtual energy level therefore; two photons should be simultaneously absorbed for this process to occur. Also TPA is directly proportional to the square of the input fluence. The propagation of laser light through the system describing the TPA is given by Eq. (3).

$$\frac{dI}{dZ} = -\alpha I - \beta I^2 \tag{3}$$

where, $\alpha$ is the linear absorption coefficient and $\beta$ is the two-photon absorption coefficient and $\sigma$ is the individual molecular two-photon absorption cross section, also

$$\sigma = \frac{\omega \beta h}{2\pi N} \tag{4}$$

where $N$ is the number of the molecules in the system and $\omega$ is the incident radiation frequency. It is the imaginary part of the third-order nonlinear susceptibility of the system that determines the strength of the two-photon absorption. The relation between the TPA coefficient and the third-order susceptibility of a centrosymmetric system for linearly polarized incident light is given as,

$$\beta = \frac{3\pi}{\epsilon_0 n^2 c\lambda}\, Im\left[\chi^3{}_{xxx}(-\omega;\omega,\omega,-\omega)\right] \tag{5}$$

here, $c$ is the speed of light, $\lambda$ is the wavelength of the incident beam and $n$ is the linear refractive index [27].

### 2.3 Three-photon absorption

The transition of a ground state molecule to higher excited state by simultaneous absorption of three photons from the incident radiation is termed as three-photon absorption (3PA) [28]. It is a fifth-order nonlinear process, and the propagation equation for a medium having significant three-photon absorption is given as,

$$\frac{dI}{dZ} = -\alpha I - \gamma I^3 \tag{6}$$

where, $\alpha$ is the linear absorption coefficient and $\gamma$ is the 3PA coefficient. For acentrosymmetric system and linearly polarized light, $\gamma$ is related to the imaginary part of the fifth-order susceptibility through the following equation,

$$\gamma = \frac{5\pi}{\epsilon_0{}^2 n^3 c^2 \lambda} \, Im\left[\chi^5{}_{xxxxx}(-\omega;\omega,\omega,\omega,-\omega,-\omega)\right] \tag{7}$$

### 2.4 Reverse saturable absorption

Reverse saturable absorption (RSA) is the property of materials where the absorption of light increases with increasing incident light intensity. It is basically a two-step, sequential single-photon absorption process where, the excited atoms/molecules make a subsequent transition to higher energy levels by absorbing another single photon [28]. For steady-state condition, the intensity change of the laser beam in the nonlinear medium along its propagation direction for RSA can be expressed as,

$$\frac{dI}{dz} = -\sigma_{12}(N_1 - N_2)I - \sigma_{23}N_2 I \tag{8}$$

where, $\sigma_{12}$ is the transition crossection from the ground state to first excited state, $N_1$ is the no. of molecules in the first excited state, $N_2$ is the no. of molecules in the second excited state and $\sigma_{23}$ is the transition crossection from first excited state to second excited state.

## 3. Types of plasmon-exciton interaction

Based on the spectral overlap between the plasmonic modes and optical exciton of the organic molecules their mutual interaction mechanism is broadly classified into nonresonant and resonant interactions.

### 3.1 Nonresonant interaction

These types of interactions are further classified into refractive index-dependent interaction and plasmon enhanced fluorescence.

#### *3.1.1 Refractive index dependent*

The type of interaction between plasmonic-organic hybrids where the electronic absorption band of the organic molecule and the plasmonic resonances are far away from each other and the refractive index of the organic molecule is nearly wavelength independent (**Figure 2A**). The adsorption of organic molecules merely increases the refractive index or the dielectric constant of the nanoenvironment surrounding metal nanocrystals. Therefore, as the induced polarization charges increase, a more pronounce screening of the Columbic restoring effect leading to a red shift in the resonance band of the plasmonic nanostructures [7, 29]. A prime example of such a plasmon molecule interaction is refractive index-based sensors where, the adsorption of such organic molecules enhances the refractive index of the environment around the plasmonic nanostructures [30].

#### *3.1.2 Plasmon enhanced fluorescence*

The organic molecules which demonstrate both absorption and fluorescence emission, tend to drastically alter their fluorescence rate when hybridized with metal

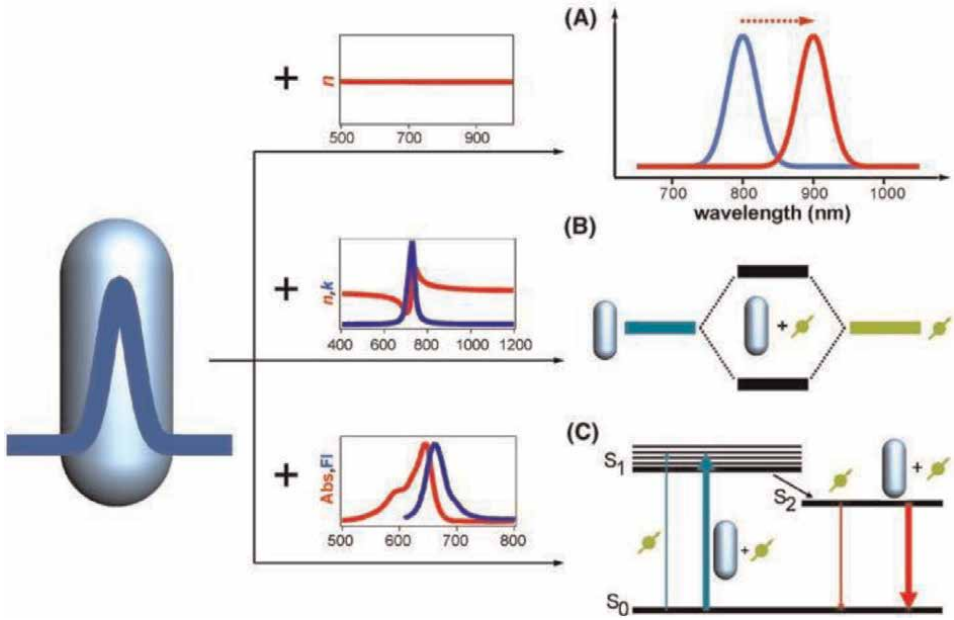


**Figure 2.**
*Schematic diagram illustrating three types of plasmon-molecule interactions. (A) Plasmon shift due to adsorption; (B) resonance coupling between metal nanocrystals and adsorbed molecules with strong absorption and (C) fluorescence enhancement when fluorophores are adjacent to metal nanocrystals [29].*

nanostructures [29, 31]. Primarily, the enhancement in the fluorescence of the organic molecule may be due to an increase in the excitation rate of the electrons from ground state to the excited state which happens due to the strengthening of the local electric field in the vicinity of the metal nanosurfaces. On the contrary fluorescence enhancement may also be attributed to the increase in electronic radiative emission from the excited states to the ground state owing to aggregation of photonic states around the metal nanostructures [7, 32]. In both these phenomena, the distance between the fluorophore and the plasmonic structure plays a key role. Novotny et al. demonstrated that organic fluorophores when conjugated with metal nanoparticles displaying intense local field enhancements then the radiative decay rate dominates the nonradiative decay rate and fluorescence enhancement takes place which further reduces the average lifetime of the organic molecule [33]. Moreover, due to the coupling with the plasmon resonance, the emission direction as well as the spectral shape of fluorophores can also be modified [34–36]. All of these open up new approaches for manipulating light at the nanoscale.

### 3.2 Resonant interactions between plasmons and excitons

Resonant coupling takes place if the absorption band of the organic molecules and the LSPR frequency of the metal nanoparticles overlap with each other. Plasmons when resonantly excited, amplify the local electric multiple times in magnitude. In such a case the coupling between the plasmonic resonances and the degenerate energy levels of the organic molecule leads to hybridized molecular states [7, 29, 31]. Based on the perturbations in the wave functions of the plasmons and, the interaction between them can be classified into weak, strong and extreme coupling [1, 37, 38]. If the wave

functions remain unaltered it is called weak coupling, origination of new dispersion relations due to the formation of hybrid states is referred to as strong coupling regime whereas, in the extreme coupling the resonance exchange energy oscillates between the upper and lower energy levels leading to a split in the absorption band [1, 39].

Pockrand et al. and Glass et al. in 1980 first demonstrated the resonance coupling effect between plasmons and excitons both theoretically and experimentally [40, 41]. Later, it was realized that the ultraviolet and visible light could switch the resonant coupling between the dye molecules and excitons this led to efficient switching with power density ~6.0 mW/cm$^2$ and switching power 0.72 nW/device [42]. Since then, efforts to decipher interaction mechanisms between strongly coupled plasmons and excitons have gained a lot of interest amongst researchers. Wiederrecht et al. first reported literature on coherent coupling between a J-aggregated molecular dye and noble metallic nanospheres (**Figure 3**) [43].

They demonstrated that the interaction between plasmons and excitons is strongly dependent on the properties of the metal nanostructure. The J-aggregated dye when hybridized with Ag nanocrystals lead to an increased absorption whereas the absorption decreased when integrated with Au nanocrystals [43]. Further, Fofang et al. investigated wavelength-dependent coupling between the J-aggregates of dye 2,2′-dimethyl-8-phenyl-5,6,5′,6′-dibenzothiacarbocyanine chloride. Their study claims that the plasmonic resonances can be tuned over a wide spectral range when strongly coupled with a metal nanostructure. In fact, the coupling energy diagram of 2,2-dimethyl-8-phenyl-5,6,5,6-dibenzothiacarbocyanine chloride and Au nanoshells hybrids depicted both asymmetric energy splitting and an anticrossing behavior [1]. The anticrossing behavior amongst resonantly coupled hybrids of Au nanorods and various other organic dyes have also been reported [44–47]. One of the major applications demonstrated by resonantly coupled plasmons and organic dyes is ultrasensitive detection of analytes. Where, resonant binding amongst Ag nanoparticles, camphor and cytochrome P450cam protein (CYP101) demonstrated a plasmon shift of up to 104 nm [48, 49]. Therefore, a complete understanding of the resonance coupling effects between plasmonic nanostructures and excitonic

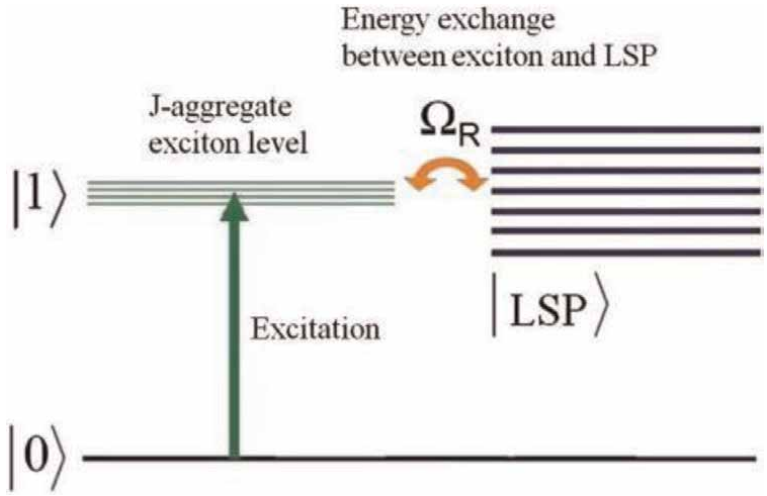


**Figure 3.**
*Schematic diagram of optical transitions in metal-J aggregate hybrid nanostructures.*

molecules is of utmost importance for realizing active photonic devices such as optical switches, lasers and energy transfer-based sensors [50].

Since, these interactions between plasmons and excitons cannot be explained by the dielectric function therefore, it was realized that energy transfer plays a vital role in delineating the characteristics of the hybrid states.

### *3.2.1 Exciton-plasmon resonant energy transfer mechanisms*

An optically excited excitonic molecule placed in the vicinity of a plasmonic nanostructure may result in an energy transfer *via* radiative or nonradiative channel.

Owing to the physical and chemical conditions the probabilistic resonant interactions between the plasmonic-organic hybrids can be due to Dexter energy transfer (DET), exciton plasmon resonance energy transfer (EPRET), Foster resonance energy transfer (FRET), nanometal surface energy transfer (NSET), metal enhanced fluorescence (MEF), enhancement of absorption cross section (lightening rod effect), enhanced photostability, and the increase of excitation rate [51].

The origin of metal enhanced fluorescence is understood in terms of the increase in optical density of states of the emitter when placed near a metal nanosurface, due to the local confinement of the incident electric field [52, 53]. This in accordance with Purcell effect which leads to an increase in the radiative decay rate of the organic molecule due to a decrease in the volume of the cavity [54].

Further, MEF is extremely sensitive to the orientation of the exciton and nanoparticle (**Figure 4**).

Both experimental and theoretical studies infer that it is the orientation of the exciton and plasmonic dipoles in MEF due to which the net luminance of the hybrid quenches or strengthens.

A radiation less energy transfer from excited state donor to ground state acceptor via long range dipole-dipole interactions is termed as FRET [55, 56].

The efficiency of this energy transfer critically depends on various factors such as the distance of separation between the acceptor and donor molecule, their spectral overlap and their emission quantum yield (QY) [57, 58]. **Figure 5** illustrates the Jablonski Diagram of this mechanism.

FRET plays an important role in the determination of sub-microscopic separations amongst interactive molecules [59, 60]. The dipole-dipole interaction between the

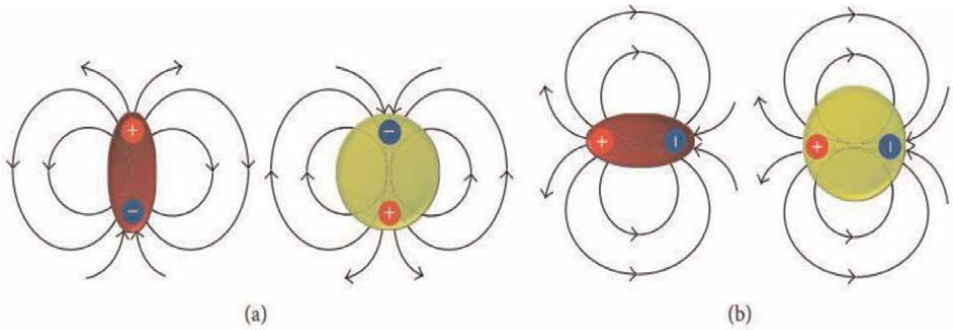


**Figure 4.**
*(a) Parallel (tangential) and (b) perpendicular (radial) orientation of chromophore dipole moment to the surface of spherical nanoparticles leading to the suppression or enhancement of the radiative decay rate of the exciton, respectively [51].*

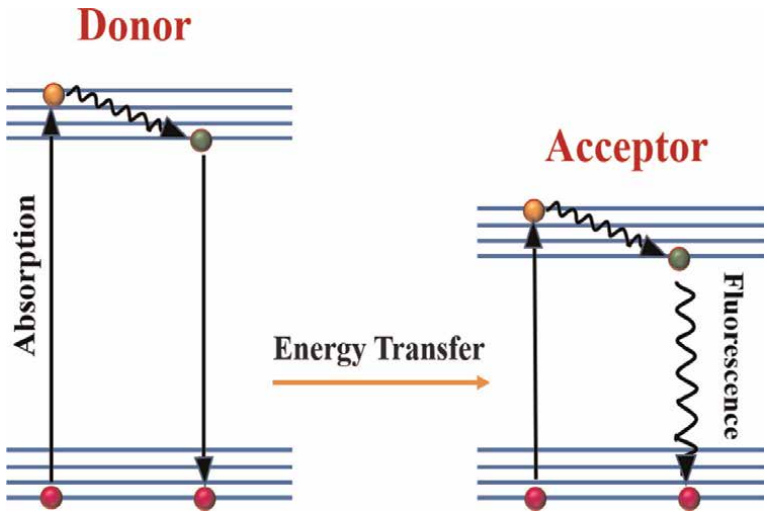


**Figure 5.**
*Jablonski diagram illustrating FRET [59].*

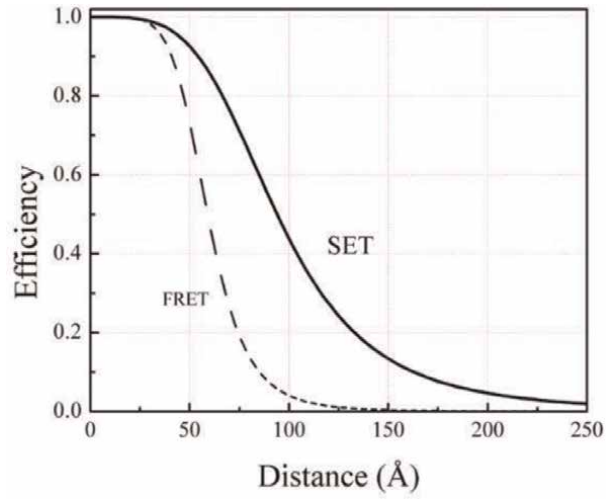


**Figure 6.**
*Comparison of energy transfer efficiency between FRET and NSET [19].*

excited donor molecule (D) and the ground state acceptor molecule (A) results in a nonradiative energy exchange between them in this occurrence. Because the energy transfer efficiency is inversely related to the sixth power of the distance between the donor and acceptor molecules, the length scale of nanoscopic FRET is limited to 8 nm beyond which it is too weak to be used [60]. Further, a long-range dipole-surface contact mechanism based on NSET has recently been developed, with energy transfer range twice that of FRET (**Figure 6**) [19, 29]. In metal nanoparticles, the rate of energy transfer from the oscillating dipole to the continuum of electron-hole pair excitations is inversely proportional to the fourth power of the donor to acceptor distance [61, 62].

In the linear regime, both FRET and NSET have been extensively recognized as an efficient tool for the determination of the distance between the sub-microscopic particles and in predicting the dynamics of a coupled hybrid [29, 63, 64].

EPRET, on the other hand, is a nonradiative dipole-dipole resonant interaction discovered by Forster. The various parameters on which EPRET critically depends are inter-particle distance between the donor and the acceptor, spectral overlap between the excitonic emission band and their plasmonic absorption band, relative orientation of the dipole moments of the organic molecule with respect to the plasmonic modes, strength of transition dipole moment, the morphology of plasmonic nanostructures and concentration and molar extinction coefficient of the plasmonic and organic molecules [51, 65]. A significant contrast between FRET and EPRET is in terms of relative orientation amongst dipoles of the donor and acceptor pair. FRET is forbidden when the dipoles are perpendicular to each other while it is maximum in case of parallel dipoles whereas, for EPRET, the probability of energy transfer is minimum when the relative orientation of the dipoles of the donor acceptor pair is perpendicular to each other, but it is never zero [51].

When the plasmon and exciton are placed very close to each other (5–10 nm) it is found that DET dominates the interaction. This type of energy transfer occurs due to hoping of electrons between the overlapping wave functions of the donor and acceptor molecule [66]. Photo-stability occurs when the short-lived excited states reduce the potential of photo-bleaching and other interactions that would otherwise destroy the chromophores' fluorescent nature, resulting in an increase in their photo-stability [51]. Furthermore, because more excited molecules are now pushed down to the ground state and ready to absorb and participate in the emission process, this impact raises the molecules excitation rate, resulting in an increase in the overall emission rate [67]. Another effect which is in closely related is the lightning rod effect and it takes place when the absorption band of the chromophore overlaps with the plasmon band of the nanoparticle. In this phenomenon, the plasmon band of the nanoparticle acts as a receiver nanoantenna and confines the electromagnetic field, and this significantly strengthens the excitation rate of the chromophore and thus enhances the total emission rate [51].

## 4. Experimental realizations

With an aim to circumvent the material bottleneck limitations hindering the realization of an on chip all optical switch, our experimental work presents a detailed insight into the morphology directed third order NLO properties of four distinct gold nanoshapes and their hybrids with an organic fluorescent dye Eosin Yellow (EY). The ultrafast structural dynamics of the gold nanoshapes and their hybrids has been delineated in terms of their spectral and temporal modulations to deconvolute the excited state dynamics responsible for the coupling between the transient states of gold nanoshapes and various intermediate states of the Eosin Yellow photocycle. Finally, the work is concluded with a mechanistic interpretation of the observed phenomenon in terms of the energy transfer within the hybrids.

In our investigations, colloidal gold nanoshapes were synthesized using chemical reduction method (**Figure 7**) while, the DC sputtering technique has been employed for fabricating the gold nanoislands film [67, 68].

Apart from this, films of Eosin Yellow having different concentrations were spin coated on a glass substrate. The shape and lattice parameters of colloidal gold

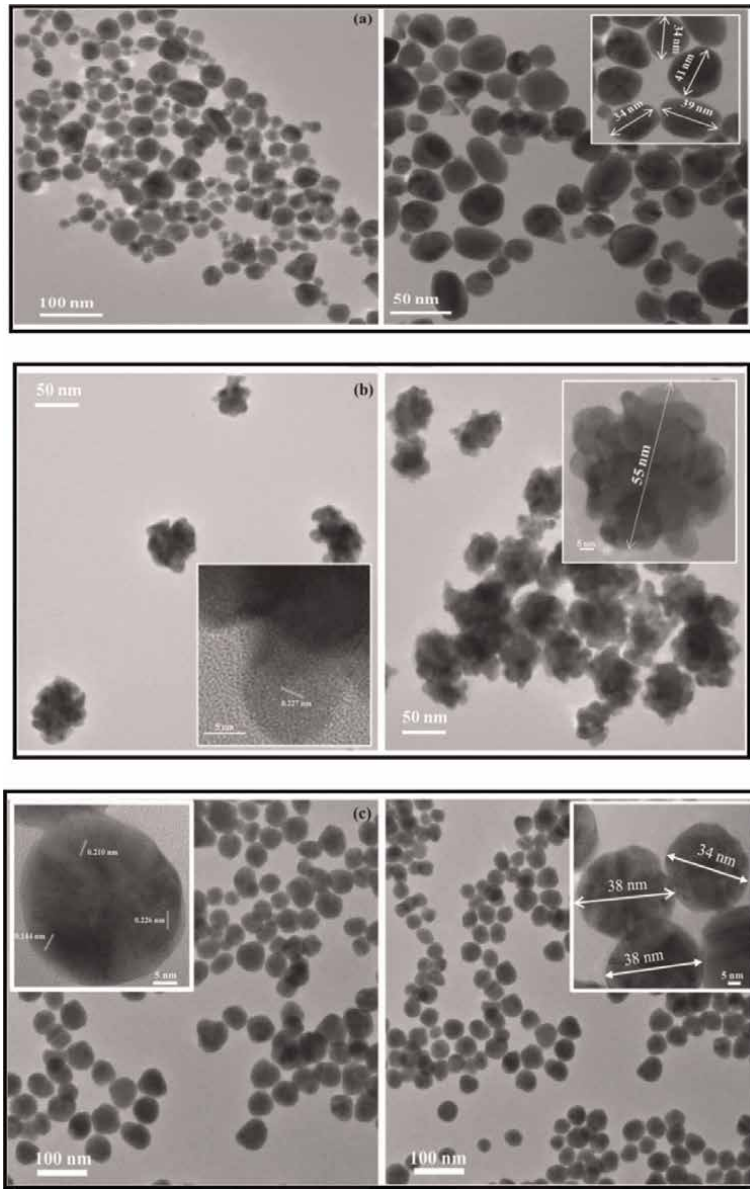


**Figure 7.**
*TEM micrographs (a) GNP (gold nanopebbles); (b) GNF (gold nanoflowers) and (c) GNS (gold nanospheres). While, the insets represents the HR-TEM image of the corresponding nanoparticles [67].*

nanostructures were estimated using high resolution transmission electron microscopy (HRTEM) and X-ray diffraction (XRD) respectively. Atomic force microscopy (AFM), field-emission scanning electron Microscopy (FESEM) and near field scanning optical microscopy (NSOM) were employed to examine the morphology of the epitaxial gold film and its interaction with the organic counterpart respectively **Figures 8–10** [67, 68].

Further, various standard spectroscopic characterizations namely absorption spectroscopy (UV-Vis), surface enhanced Raman spectroscopy (SERS), third order

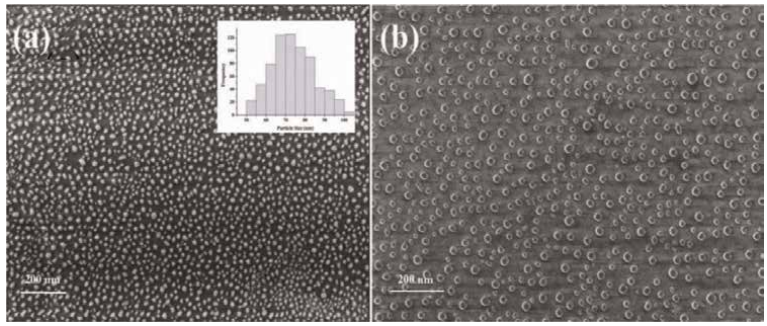


**Figure 8.**
*FESEM image of (a) gold Nanoislands film at high magnification (inset represents the particle size distribution) and (b) EY-gold nanoislands hybrid [68].*

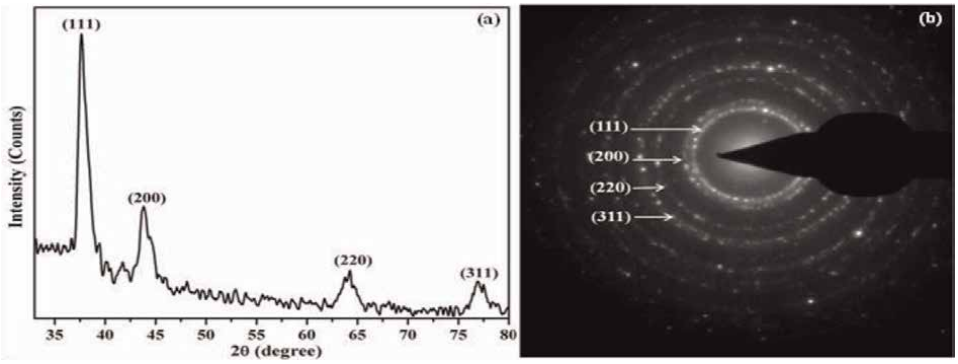


**Figure 9.**
*(a) Powder X-ray diffraction pattern and (b) selected area electron diffraction pattern of Au colloids demonstrating FCC structure [67].*

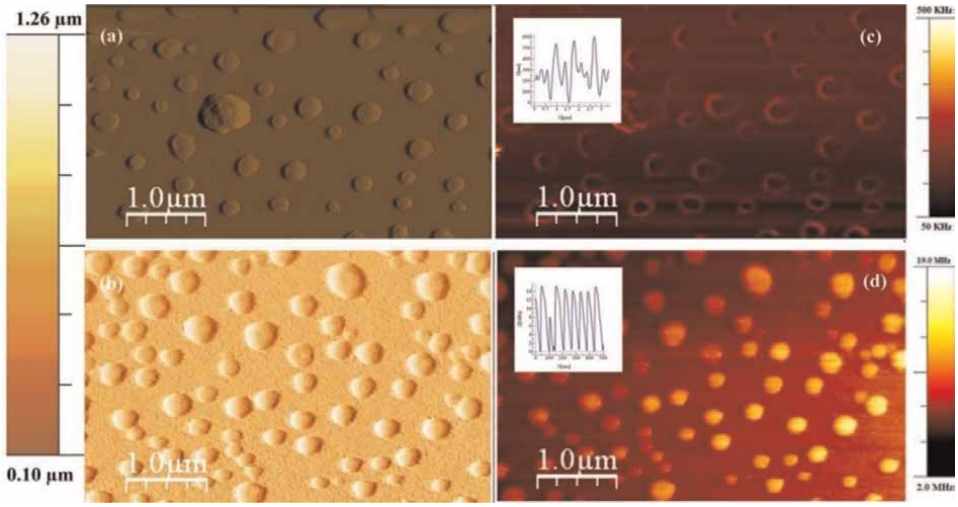


**Figure 10.**
*(a, b) AFM representation of bare Au-islands and EY-Au islands hybrid, respectively and (c, d) 2-D NSOM image of the raw gold nanoislands and EY-Gold nanoislands film, respectively (inset represents the intensity of field in terms of oscillation with maxima and minima in the x–z plane) [68].*

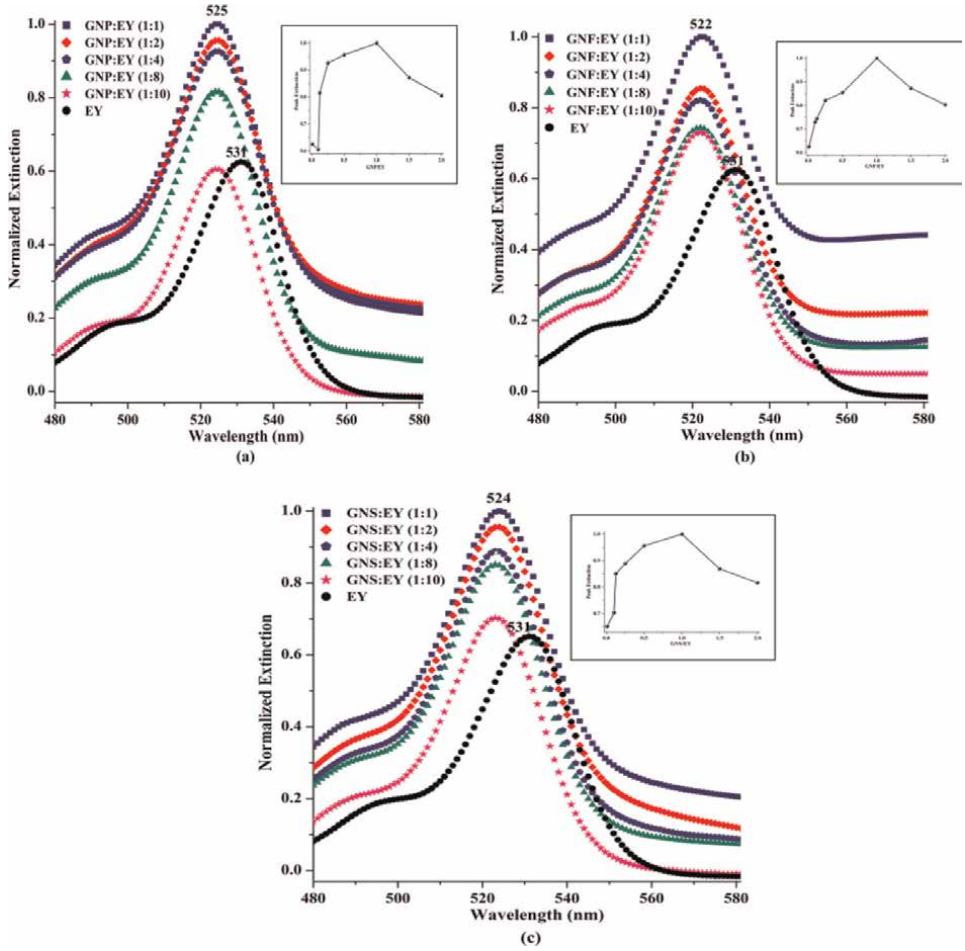


**Figure 11.**
*Normalized extinction spectra of free Eosin Yellow (EY) and its hybrid with (a) GNP; (b) GNF and (c) GNS. The insets represent peak extinction maxima (normalized w.r.t 1:1 (v/v) gold nanoparticles-EY ratio) of the hybrid structures [67].*

nonlinear spectroscopy (Z-Scan), photoluminance spectroscopy (PL) and ultrafast time resolved pump probe spectroscopy (UTRPPS) have been used to unveil the steady state as well as the excited state dynamics of all four distinct gold nanoshapes and their hybrids with EY (**Figures 11–14**). For a detailed explanation regarding the synthesis, experimental setups employed and the experimental results the corresponding papers may be referred [67–69].

## 5. Conclusions of the experimental analysis

The linear absorbance, nonlinear absorption coefficient and nonlinear refractive index measurements of the four distinct plasmonic shapes, namely colloidal gold nanoflowers, colloidal gold nanopebbles colloidal gold nanospheres and gold nanoislands film confirmed that not only size but the geometry of the plasmonic structures plays a vital role in determining their linear as well as nonlinear optical

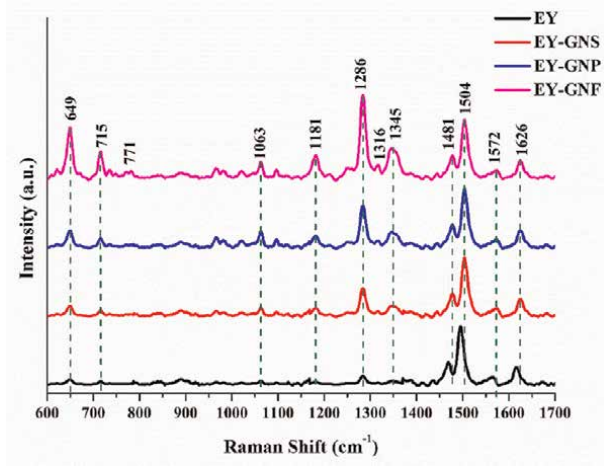


**Figure 12.**
*(a) Raman spectra of Eosin Yellow dye and its hybrids illustrating morphology directed SERS effect [68].*

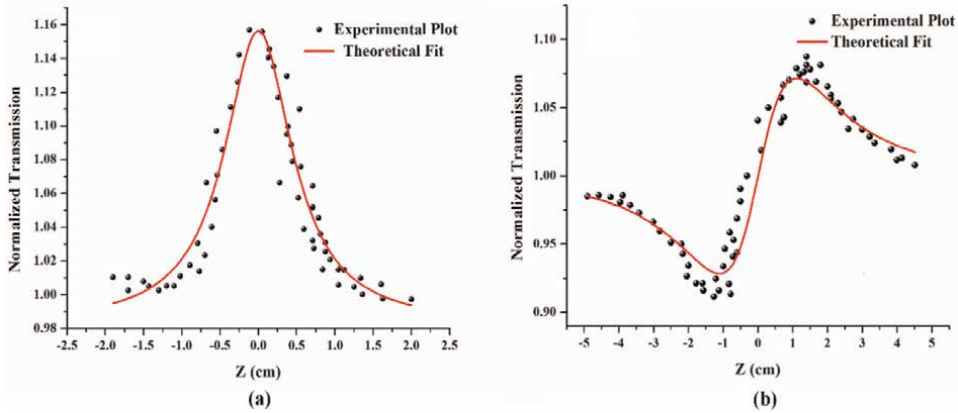


**Figure 13.**
*Z-scan representation of Eosin Yellow dye (a) open aperture and (b) closed aperture scan [67].*

coefficients. A strong mutual interaction between the organic dye Eosin Yellow and plasmonic structures has been inferred from the Raman spectroscopic analysis. Further, the observed results deduce that the nanostructures with sharp edges, offering plenty of hotspots, may be competitive candidates for highly sensitive SERS probes. Nonlinear transmission measurements of colloidal plasmonic shapes, organic fluorophore EY and their colloidal plasmonic organic hybrids show that they possess excellent saturable absorption properties at 532 nm wavelength. Further, the Two Photon Absorption coefficients reported for colloidal plasmonic organic hybrids reveal that the enhancement induced by the plasmonic structures in the in the third order nonlinearity of the organic dye Eosin Yellow critically depends on the morphology of the plasmonic structures. Further, the results based on the spectral and temporal modulations of EY hybrids in solution and film demonstrated that the excitonic states of molecular hybrids tend to modify drastically due to strong coupling between molecular excitons and plasmons. The energy transfer mechanism delineated for all the four EY-gold nanoshapes hybrids depicts that Forster resonance energy transfer

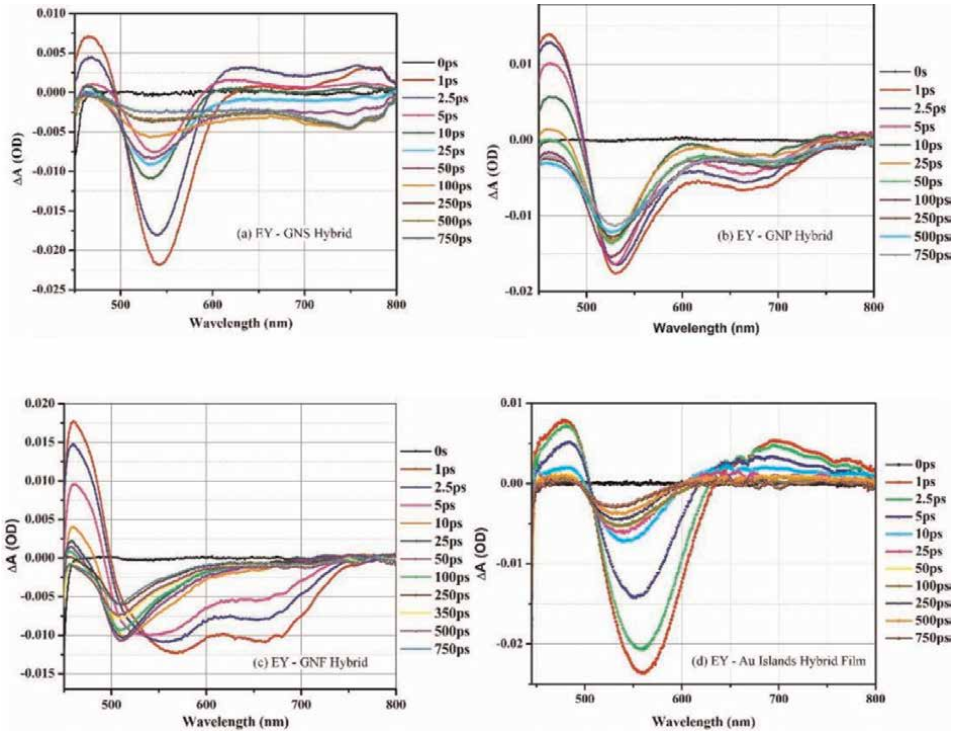


**Figure 14.**
*Transient absorption spectra at various time delays measured for EY when hybridized with (a) colloidal gold nanospheres; (b) colloidal gold nanopebbles; (c) colloidal gold nanoflowers and (d) nanoislands film pumped at visible wavelength (420 nm, power = 1.5 mW) [69].*

(FRET) took place between EY-GNS, EY-GNP and EY-Au islands while nanometal surface energy transfer (NSET) existed between EY-GNF.

These findings may find importance in fabrication of energy transfer based active photonic devices.

## 6. Summary

The work reported herein, presents a significant enhancement in the third-order nonlinearity of a technologically promising organic dye Eosin yellow (EY) when hybridized with three distinct colloidal gold nanoshapes, namely, gold nanospheres (GNS), gold nanopebbles (GNP) and gold nanoflowers (GNF) and a gold nanoislands film (Au islands). Indeed, up to 400% increase in the NLO response of EY when hybridized with Au islands was demonstrated when excited with a 532 nm, 20 ps laser. Further, a 50% reduction in the response time been attained. Herein, the role of resonant interactions within the hybrids especially in terms of nonradiative energy in altering the steady state as well as excited state dynamics due to the spectral overlap between the extinction spectra of the gold nanoshapes and the emission spectra of the dye has been emphasized. Finally, a descriptive uncertainty budget for the precise measurement of the third order NLO coefficients has been documented.

Based on the hypothesis that the nonradiative energy transfer has the ability to significantly alter steady state as well as excited state dynamics of plasmonic organic

hybrids and a unique relationship exists between the efficiency of energy transfer and the enhancement in the third order NLO coefficients, this study may be safely extended to a wide range of energy transfer-based plasmonic-organic hybrids.

## Acknowledgements

The authors are thankful to the Department of Physics and Astrophysics, University of Delhi, Delhi 110007, India, for granting permission to publish this work. Kaweri Gambhir acknowledges financial support from Dr. D. S. Kothari Postdoctoral Research Fellowship, University Grant Commission, India, through Grant No. No. F.4-2/2006 (BSR)/PH/19-20/0097.

## Author details

Kaweri Gambhir* and Agnikumar G. Vedeshwar
Thin Film Laboratory, Department of Physics and Astrophysics, University of Delhi, Delhi, India

*Address all correspondence to: kawerigambhir@gmail.com